A Multi-objective Approach to Solve the Build Orientation Problem in Additive Manufacturing

Marina A. Matos[1], Ana Maria A. C. Rocha[1], Lino A. Costa[1], and Ana I. Pereira[2(✉)]

[1] ALGORITMI Center, University of Minho, 4710-057 Braga, Portugal
aniram@live.com.pt, {arocha,lac}@dps.uminho.pt
[2] Research Centre in Digitalization and Intelligent Robotics (CeDRI), Polytechnic Institute of Bragança, 5300-253 Bragança, Portugal
apereira@ipb.pt

Abstract. Additive manufacturing (AM) has been increasingly used in the creation of three-dimensional objects, layer-by-layer, from three-dimensional (3D) computer-aided design (CAD) models. The problem of determining the 3D model printing orientation can lead to reduced amount of supporting material, build time, costs associated with the deposited material, labor costs, and other factors. This problem has been formulated and studied as a single-objective optimization problem. More recently, due to the existence and relevance of considering multiple criteria, multi-objective approaches have been developed.

In this paper, a multi-objective optimization approach is proposed to solve the part build orientation problem taking into account the support area characteristics and the build time. Therefore, the weighted Tchebycheff scalarization method embedded in the Electromagnetism-like Algorithm will be used to solve the part build orientation bi-objective problem of four 3D CAD models. The preliminary results seem promising when analyzing the Pareto fronts obtained for the 3D CAD models considered. Concluding, the multi-objective approach effectively solved the build orientation problem in AM, finding several compromise solutions.

Keywords: Additive manufacturing · 3D printing · Multi-objective optimization · Build orientation

1 Introduction

Additive manufacturing (AM) processes involve the use of three-dimensional (3D) computer-aided design (CAD) data to create physical models. Typically, AM is characterized by four processing stages: model orientation, creation of supports, slicing, and path planning [17]. AM allows the production of a wide range of shapes, with very complex geometries and not requiring many post-processing

© Springer Nature Switzerland AG 2019
S. Misra et al. (Eds.): ICCSA 2019, LNCS 11621, pp. 261–276, 2019.
https://doi.org/10.1007/978-3-030-24302-9_19

actions. The layered manufacturing processes apply physical or chemical phenomena to construct parts, adding layer-by-layer material. This type of manufacture began in the years 80 by Kruth [10]. Currently, layered manufacturing processes are used in several areas such as medical sciences (e.g. dental restorations and medical implants), jewelry, footwear industry, automotive industry and aircraft industry [16].

Over the years, the adoption of Rapid Prototyping (RP) technologies to fabricate a prototype model from a CAD file has grown and has been implemented in many model manufacturing companies due to its effectiveness in the prototype model development at a reduced time [2]. The performance of an RP depends on the orientation of the parts on the printer platform, that is, each piece must have the correct orientation in order to improve the surface quality, minimize the number of support structures and minimize the manufacturing time [19].

The automatic selection of the best orientation manages to reduce or eliminate errors involved throughout the model construction process [22]. The selection of the best orientation is a very important factor because affects the time and print quality, amount of supporting material, shrinkage, distortion, resin flow, material cost, volume and support area and has a better precision of the model [16,23]. Several approaches have been carried out to determine the orientation of a model based on single-objective optimization. Usually the objective functions used for optimal build orientation were the build height, staircase effect, volumetric error, volume of support structures and part area in contact with support structures, surface quality, surface roughness and build deposition time [2,3,11,14,18,19,22].

Recently, multi-objective approaches have been developed to determine the optimal object building orientation, essentially by reducing the multi-objective problem to a single-objective one using classical scalarization methods such as the weighted sum method. Cheng et al. [4] formulated a multi-objective optimization problem focused on the surface quality and production cost of the parts, obtaining solutions for all types of surfaces, whether with complex geometries or not, or even for curved surfaces. The Particle Swarm Optimization (PSO) algorithm was used in [12] to solve a multi-objective optimization problem in order to get the desired orientations for the support area, build time and surface roughness. A multi-objective optimization approach considering as objective functions the surface roughness and the build time, for different models, was developed by Padhye and Deb in [15]. They used the NSGA-II (Non-dominated Sorting Genetic Algorithm) and MOPSO (Multi-Objective Particle Swarm Optimization) algorithms to obtain the Pareto front. Gurrala and Regalla [7] applied the NSGA-II algorithm to optimize the strength of the model and its volumetric shrinkage as objective functions. They concluded, through the Pareto front, that with the shrinkage of the part its strength increases in the horizontal and vertical directions. A genetic algorithm was used in [1] for solving a multi-objective build orientation problem. They optimized several variables, yield and tensile strength, elongation and vickers hardness, for material properties used, surface roughness, support structure and build time and cost.

In this paper, we propose a multi-objective optimization approach to optimize the support area and the build time in order to get the best orientation of 3D CAD models using the Electromagnetism-like algorithm combined with weighted Tchebycheff scalarization method is proposed. The weighted Tchebycheff method was selected since it can be used to solve problems with nonconvex Pareto fronts and can find non-extreme solutions (trade-offs) in the presence of multiple conflicting criteria. Four models previously used in a single-objective context will be used [19].

This paper is organized as follows. Section 2 introduces the build orientation optimization problem and the multi-objective optimization approach used in this study. The description of the models used in the numerical experiments, the Pareto fronts obtained for each model as well as an appropriate discussion for each one is presented in Sect. 3. Finally, Sect. 4 presents the conclusions of this study and the future work.

2 Optimization Problem

2.1 Part Orientation

The surface finish of an object obtained through additive manufacturing process is highly important. A good surface finish can decrease or even eliminate time spent in subsequent post-processing (finishing). Part orientation can affect the surface finish due to the slicing process and the support material usage in the build of the part. Rotating a part to a different orientation can decrease the support usage and build time of a part.

One of the problems affecting the surface finish of the part is the staircase effect. The layer thickness have an impact on the staircase effect, since the smaller the thickness of the model layer the staircase effect will also be smaller, resulting in a better surface finish. This effect is related to the cusp height (CH) that is based on the maximum distance between the part surface and the model surface [13] (see Fig. 1). The CH is given by $CH = t\cos(\theta)$, where t is the layer thickness and θ is the angle between the part surface and the CH.

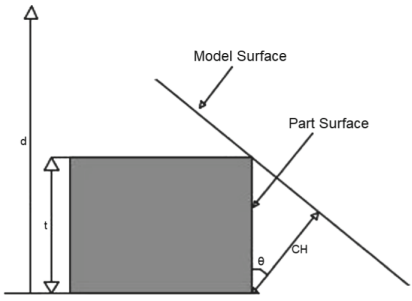

Fig. 1. Cusp height

In addition, the CAD model area is also very important for the construction of the part. For some functions, a direction vector d is required and is calculated by $x^2 + y^2 + z^2 = 1$, where the variables x, y, and z are given by (1):

$$d = \begin{cases} x = \sin\beta \times \cos\alpha \\ y = \sin\beta \times \sin\alpha \\ z = \cos\beta \end{cases} \tag{1}$$

Figure 2 shows the unit direction vector d with the variables represented.

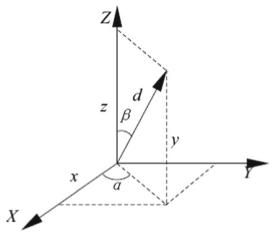

Fig. 2. Unit direction vector of build orientation [9].

2.2 Objective Functions

There are different measures that can be considered to determine the best build orientation for an improvement of the surface finish. Some of them take into account factors as the part accuracy, building time, structure support and part stability. The build orientation of a model can improve the accuracy of the part and reduce the number of generated supports, and consequently decrease the final building costs. At the same time, the construction/build time should be reduced in order to decrease the final building costs too. Thus, in this study a multi-objective optimization to determine the build orientation of a 3D CAD model according to two factors: the support area and the build time will be used.

The support area is defined as the total area of the downward-facing facets, that is, the quantity of supports to be used in the construction of the part, measured through the total contact area of the external supports with the object. In fact, the support area mostly affects post-processing and superficial finish [9,19].

The support area (SA) can be defined by

$$SA = \sum_i A_i \ \left|d^T n_i\right| \ \delta \tag{2}$$

$$\delta = \begin{cases} 1, & \text{if } d^T n_i < 0 \\ 0, & \text{if } d^T n_i > 0 \end{cases}$$

where A_i is the area of the triangular face i, d is the unit vector of the direction of construction of the triangular face i, n_i is the normal unit vector of the triangular

face i and δ is the initial function [9]. In this study, it was considered the vector $d = (0, 0, 1)^T$ to be the direction of slicing after a rotation along the angles (x, y), taking into account that each angle is between 0 and 180°.

The build time includes the scanning time of the solid, the scanning time of the solid contours and the scanning time of the support needed for the part, where the scanning times of the solid and its contours are independent of the construction direction, and the scanning time of the support depends on your volume.

The preparation time of the piece encompasses the precise time for the platform to move downwards during the construction of each layer, the scraping time of this and other times of preparation of the part. This time depends on the total number of slices of the solid, the number of slices dependent on the height of the construction direction of a particular part of the piece. Therefore, minimizing this height and the number of layers, can decrease the construction time of the part [9,19].

The build time (BT) is given by (3):

$$BT = \max(d^T v_1, d^T v_2, d^T v_3) - \min(d^T v_1, d^T v_2, d^T v_3) \tag{3}$$

where d is the direction vector and v_1, v_2, v_3 are the vertex triangle facets.

2.3 Multi-objective Approach

Based on the part build orientation problem, the multi-objective optimization intends to simultaneously minimize the support area and the build time, defined in Eqs. (2) and (3). The general multi-objective optimization problem is formulated as

$$\begin{aligned} &\min\ f(\theta_x, \theta_y) = \{f_1(\theta_x, \theta_y), f_2(\theta_x, \theta_y)\} \\ &\text{s.t.}\ \ 0 \leq \theta_x \leq 180 \\ &\qquad 0 \leq \theta_y \leq 180 \end{aligned} \tag{4}$$

where the objective functions $f_1(\theta_x, \theta_y)$ and $f_2(\theta_x, \theta_y)$ are, respectively, the support area, SA in (2), and the part building time, BT in (3). In this problem, the θ_x and θ_y are the rotation along the x-axis and the y-axis, respectively.

Approximating the Pareto optimal set is the main goal of a multi-objective optimization algorithm. A first attempt to solve this problem is to reformulate the multi-objective optimization problem to a single-objective one using a scalarization method in order to obtain different trade-offs between the objectives [8]. In scalarization methods, weights and/or goals are introduced. The simplicity is the main advantage of the weighted sum method based on the linear combination of the objectives. However, in the case of problems with nonconvex fronts, it is not possible to find non-supported solutions since there is no weights yielding these elements of the Pareto set.

In this paper, the weighted Tchebycheff scalarization method will be applied since it is suitable to tackle nonconvex problems. In this method, introduced by Steuer and Choo [21], the L_∞ norm is minimized, i.e., the maximum distance to a reference point (or aspiration levels) is minimized. This method can be

used as an a posteriori approach in which the decision making process takes place after the search. In this case, the reference point is defined as the *ideal vector* and the weights are uniformly varied to obtain different trade-offs. The ideal vector can be computed by determining the optimum of each objective. In this manner, after the search, a set of Pareto optimal solutions is presented as alternatives and the decision maker can identify the compromises and choose according to his/her preferences. A disadvantage of the weighted Tchebycheff method is, however, that in addition to the non-dominated points also weakly non-dominated points can be found [5].

The weighted Tchebycheff method is defined by:

$$\begin{array}{l} \min \max_{i=1,\ldots,k} \left[w_i (f_i(x) - z_i^\star) \right] \\ \text{s.t.} \quad x \in \chi, \end{array} \tag{5}$$

where k is the number of objective functions, w_i are the components of the weights vector, f_i is the $i-$th objective function, $z_i^\star$ are the components of the ideal vector and χ is the feasible set of the decision vectors.

Finally, the single-objective optimization problem to be solved, that resulted from a transformation of the multi-objective problem (4) through the weighted Tchebycheff scalarization method, is given by

$$\begin{array}{l} \min \max \{ w_1 (f_1(x) - z_1^\star), w_2 (f_2(x) - z_2^\star) \} \\ \text{s.t.} \quad 0 \leq \theta_x \leq 180 \\ \qquad 0 \leq \theta_y \leq 180. \end{array} \tag{6}$$

In this study, we are interested in the Electromagnetism-like (EM) algorithm, proposed in [6] and specifically designed for solving bound constrained optimization problems, to solve the problem (6). The EM algorithm is a population-based stochastic search method for global optimization that mimics the behavior of electrically charged particles. EM algorithm simulates the electromagnetism theory of physics by considering each point in the population as an electrical charge. The EM uses an attraction-repulsion mechanism to move a population of points towards optimality. The steps of the EM algorithm for bound constrained optimization are described in Algorithm 1 as shown below.

```
Randomly generate the population
Evaluate the population and select the best point
while maximum number of function evaluations is not reached do
    Compute the charges
    Compute the total forces
    Move the points except the best point
    Evaluate the new population and select the best point
end
```

Algorithm 1. EM algorithm

The EM algorithm starts with a population of randomly generated points from the feasible region. All points are evaluated (the corresponding objec-

tive function values are computed) and compared in order to identify the best point. Analogous to electromagnetism, each point in the space is considered as a charged particle. The charge of each point is related to the objective function value and determines the magnitude of attraction or repulsion of the point over the others in the population. Points with lower objective function values attract others while those with higher function values repel. The charges are used to find the total force exerted on each point as well as a direction for each point to move the points in the subsequent iterations. The total force vector exerted on each point by the other points is the sum of individual component forces, each depending on the charges. According to the electromagnetism theory, each individual force is inversely proportional to the square of the distance between the two points and directly proportional to the product of their charges. Then, the normalized total force vector exerted on the point is used to move the point in the direction of the force by a random step size. The best point is not moved and is carried out to the subsequent iteration. This process is repeated at least for a maximum number of objective function evaluations and the best point is identified as the output of the algorithm. A fully description of the EM algorithm can be found in [20].

3 Numerical Experiments

3.1 Models Description

In this section, we present the 3D CAD models that will be used. First, the CAD models should be converted into an STL (STereoLithography) format that is the standard file type used by most common 3D printing file formats. The STL files describe only the surface geometry of a 3D object, not presenting color, texture, or other common attributes of the CAD model. This represents a 3D solid object using triangular faces. The more complex the models are, the greater their number of triangular faces.

Figure 3 shows the STL files of the models that will be used in the present study, already used in a single-objective optimization study in [19]: Air Duct, Rear Panel Fixed, Rocket Shot and 45 Degree Short. Table 1 presents the data of the models studied in this work, namely the Size ($width \times height \times depth$), the volume (*Vol.*), the number of triangles (*Triangles*) and the number of slices (*Slices*) of each model. A slicing along the z-axis of 0.2 mm height was considered.

Table 1. Data of the models.

	Size (mm)	*Vol.* (cm^3)	*Triangles*	*Slices*
Air Duct	$52 \times 109.9 \times 102.5$	30.6	6024	529
Rear Panel Fixed	$142.5 \times 142.5 \times 113$	46.2	3008	676
Rocket Shot	$61.4 \times 66.9 \times 61.37$	20.8	10616	324
45 Degree Short	$157.5 \times 125 \times 157.5$	80.8	66888	625



Fig. 3. STL representation of the models.

The numerical experiments were carried out on a PC Intel(R) Core(TM)i7-7500U CPU with 2.9 GHz and 12.0 GB of memory RAM. The EM algorithm was coded in MATLAB Version 9.2 (R2017a) as well as all the optimization code developed to solve the problem (6).

3.2 Results

In order to compute the solutions of the problem (6), we used the objective functions SA in (2) and BT in (3), that were normalized using the ideal and nadir vectors. The ideal vector $z^\star$ is constructed with the individual optimal objective values, corresponding to the lower bound of each objective in the entire feasible space. The nadir vector z^{nad} represents the upper bound of each objective in the entire Pareto optimal set. Normalized values of the i-th objective function can be computed by

$$f_i^{\text{norm}}(x) = \frac{f_i(x) - z_i^\star}{z_i^{\text{nad}} - z_i^\star}.$$

The weights were uniformly varied, i.e., $(w_1, w_2) \in \{(0,1),(0.1,0.9),\ldots,(1,0)\}$. A population size of 20 and a maximum number of function evaluations of 2000 were considered for the EM algorithm. For each combination of weights, 30 independent runs were performed. In addition, the software *Simplify 3D* was used, which is a 3D model printing simulator, to show the solutions found for each model.

The Pareto fronts for the different models will be displayed. In all graphs, the solutions obtained are plotted with a blue dot and the non-dominated ones are marked with a red circle. Representative solutions will be selected to discuss the trade-offs between the objectives and identify the features associated to these solutions.

Figure 4 plots the solutions obtained in the objective space for the Rear Panel Fixed model. The table next to the Pareto front chart presents the angles and objective function values for the four representative non-dominated solutions of the Pareto front (solutions A to D). The Pareto front is nonconvex for this problem. Solutions A and D are the optimal solutions in terms of SA and BT, respectively. Solutions B and C are different trade-offs between the objectives. It is observed that solution B is little more advantageous in terms of BT in relation

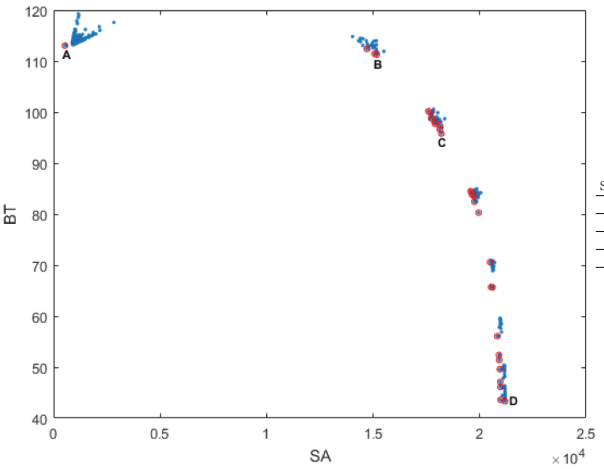

Solution	θ_x	θ_y	SA	BT
A	90.0	180.0	536.1	113.1
B	124.7	149.9	15173.0	111.3
C	139.2	142.7	18204.0	95.8
D	180.0	134.9	21189.8	43.3

Fig. 4. Pareto front and representative solutions for the Rear Panel Fixed model.

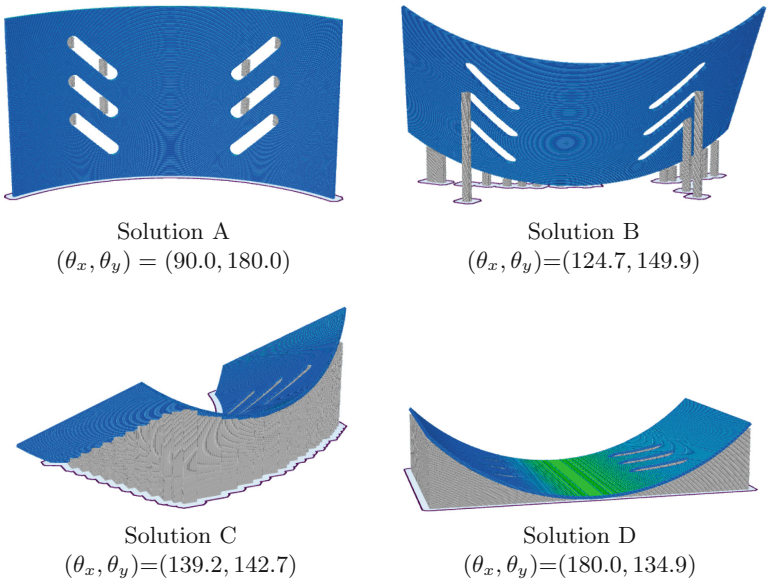

Solution A
$(\theta_x, \theta_y) = (90.0, 180.0)$

Solution B
(θ_x, θ_y)=(124.7, 149.9)

Solution C
(θ_x, θ_y)=(139.2, 142.7)

Solution D
(θ_x, θ_y)=(180.0, 134.9)

Fig. 5. Representation of the solutions A, B, C and D of Rear Panel Fixed model.

to solution A, but it is quite worse in terms of SA. When comparing solution C with solution D, a large decrease in the BT value and a small degradation in the SA value can be observed.

The 3D representations of solutions A to D can be seen in Fig. 5. Solution A, with the best value of SA and the worst value of BT, corresponds to the angles $(90.0, 180.0)$. Conversely, solution D in the other extreme of the Pareto front

has the angles (180.0, 134.9). There are other solutions that represent different compromises between the two objectives. Solution B with angles (124.7, 149.9) does not require many supports, but in terms of BT spends more time. Solution C with angles (139.2, 142.7) has a lower height (better in terms of BT), but requires many supports, as can be viewed in Fig. 5.

Figure 6 shows the Pareto front obtained for the Air Duct model and the table indicates the angles and objective function values for the six representative non-dominated solutions selected (solutions A to F). In this problem, the Pareto front is also nonconvex. Solutions A and B have similar values of BT, but solution B is significantly worse than solution A with respect to SA. This stresses the importance of identifying the compromises between the objectives. The gain in BT achieved by solution B when compared to solution A is negligible and the loss in terms of SA is large. Therefore, solution A is clearly preferable than solution B. When comparing the other compromise solutions between C and F, it is observed an improvement in terms of BT, but a degradation in the value of SA.

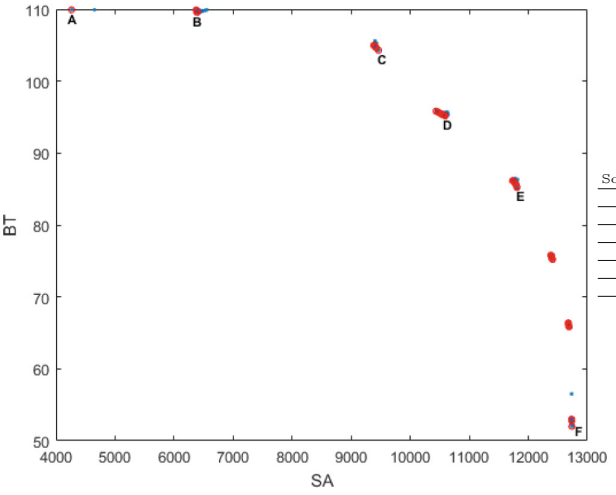

Solution	θ_x	θ_y	SA	BT
A	180.0	180.0	4264.7	109.9
B	35.1	0.1	6398.6	109.6
C	64.0	179.6	9462.0	104.3
D	72.6	23.4	10591.0	95.2
E	72.6	48.8	11807.8	85.2
F	126.2	90.0	12736.3	52.0

Fig. 6. Pareto front and representative solutions for the Air Duct model.

The 3D representations of solutions A to F for the Air Duct model are presented in Fig. 7. The best solution in terms of SA is the solution A with orientation (180.0, 180.0). The minimum value of BT is obtained with orientation (126.2, 90.0) corresponding to solution F. The remaining solutions are compromise solutions between the two objectives. In particular, solutions D and E have a similar θ_x value and a different θ_y value, where a rotation in y-axis is observed. This means that an improvement was obtained in terms of BT, since the orientation of the object to be printed led to a smaller height, but at the expense of an increase in the number of supports as can be seen in Fig. 7. The variation of θ_y allows to reduce BT from solution D to solution E (but SA increases).

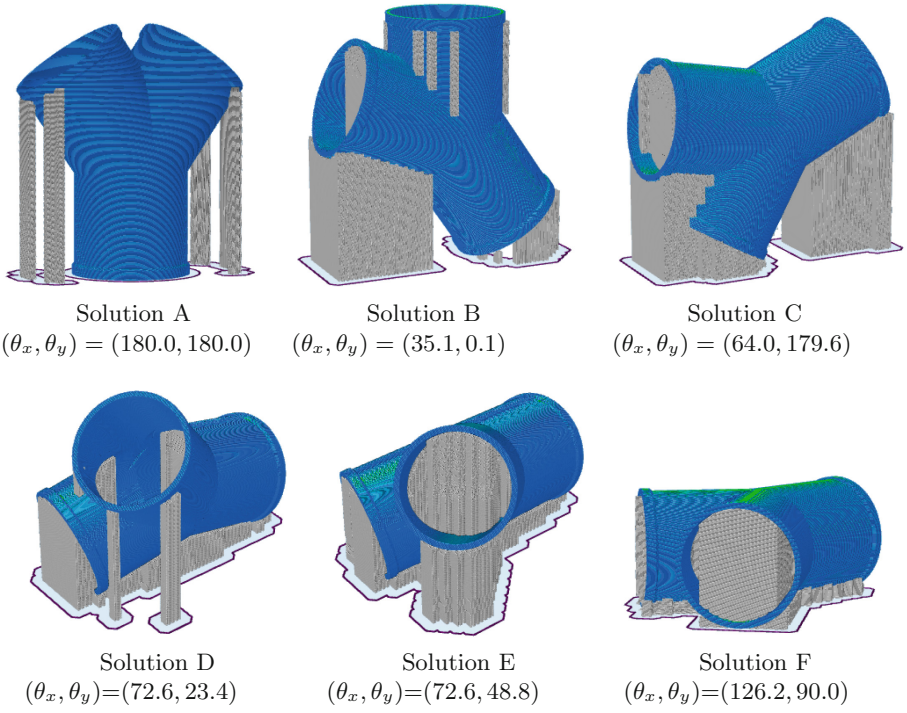

Fig. 7. Representation of the solutions A, B, C, D, E and F of Air Duct model.

Figure 8 shows the Pareto front obtained for the Rocket Shot model and the table indicates the angles and objective function values for five representative solutions (solutions A to E). Again, a nonconvex Pareto front was obtained. From the figure and the table, it turns out that solutions A and B have the same BT value. Therefore, solution A is preferable to solution B since has a better value of SA. Looking at solutions from C to E, it can be observed that, along the Pareto front, they constitute improvements in terms of BT, but worsening the values of SA. The 3D representations of solutions A to E are presented in Fig. 9. Solution A with orientation $(180.0, 180.0)$ is the best in terms of SA and has fewer brackets. Conversely, the solution E with the angles $(90.1, 135.0)$ minimizes BT but has the worst SA value. The remaining solutions are trade-offs between the two objectives. It should be noted that solution B with orientation $(180.0, 0.0)$ is similar to solution A in terms of BT, but it is worse in terms of SA. This is due to the fact that rotating the solution A by 180° in the y-axis corresponds to a solution with the same height. The solution D with orientation $(104.6, 135.0)$ when compared to solution C with orientation $(97.9, 90.0)$ improves significantly in terms of BT with a small degradation of the value of SA, as it can be seen in Fig. 9.

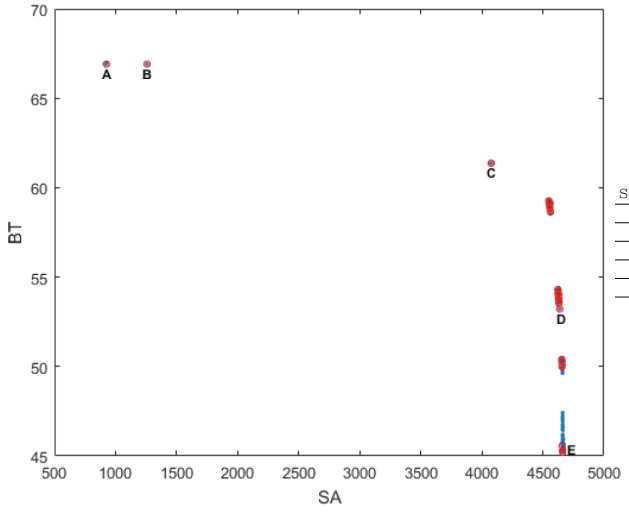

Solution	θ_x	θ_y	SA	BT
A	180.0	180.0	924.4	66.9
B	180.0	0.0	1258.8	66.9
C	97.9	90.0	4077.1	61.4
D	104.6	135.0	4637.5	53.2
E	90.1	135.0	4661.3	45.2

Fig. 8. Pareto front and representative solutions for the Rocket Shot model.

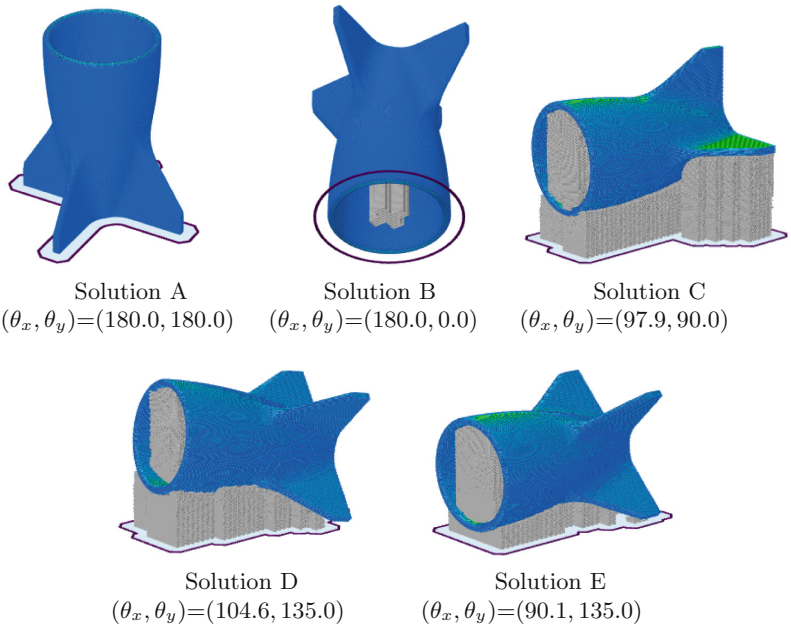

Fig. 9. Representation of the solutions A, B, C, D and E of Rocket Shot model.

In Fig. 10, it is presented the Pareto front obtained for the 45 Degree Short model as well as the corresponding angles and objective function values for the four representative non-dominated solutions (solutions A to D). As it can be seen, the Pareto front has some nonconvex regions. Solution A is the solution with the best SA value. Solution B represents a large improvement of the value of BT when compared to solution A. However, this implies some degradation of the SA value. Between solutions B and D there is a significant increase in SA and a slight reduction in the value of BT. Thus, solution B seems to be a good compromise between SA and BT. Solution D is the solution with the best BT value but with a large value of SA.

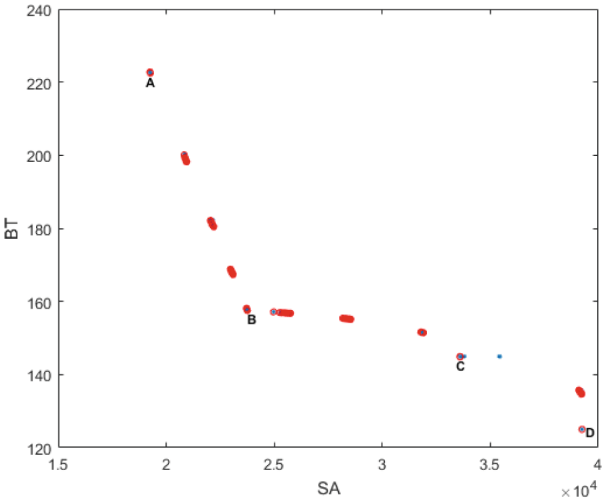

Solution	θ_x	θ_y	SA	BT
A	89.9	135.3	19246.3	222.7
B	175.8	90.0	23755.4	157.5
C	91.6	45.0	33597.0	144.9
D	0.0	0.0	39241.8	125.0

Fig. 10. Pareto front and representative solutions for the 45 Degree Short model.

The 3D representations of solutions A to D are presented in Fig. 11. Solution A with the angles $(89.9, 135.3)$ has the best SA value, but the worst BT value. On the other extreme of the Pareto front, solution D with orientation $(0.0, 0.0)$ has the best value of BT, since its orientation reduces the height of the model. However, this solution has the worst SA value since many supports are required. Solutions B and C with the angles $(175.8, 90.0)$ and $(91.6, 45.0)$, respectively, are compromise solutions between BT and SA. Solution C is better in BT and worse in SA when compared to solution B.

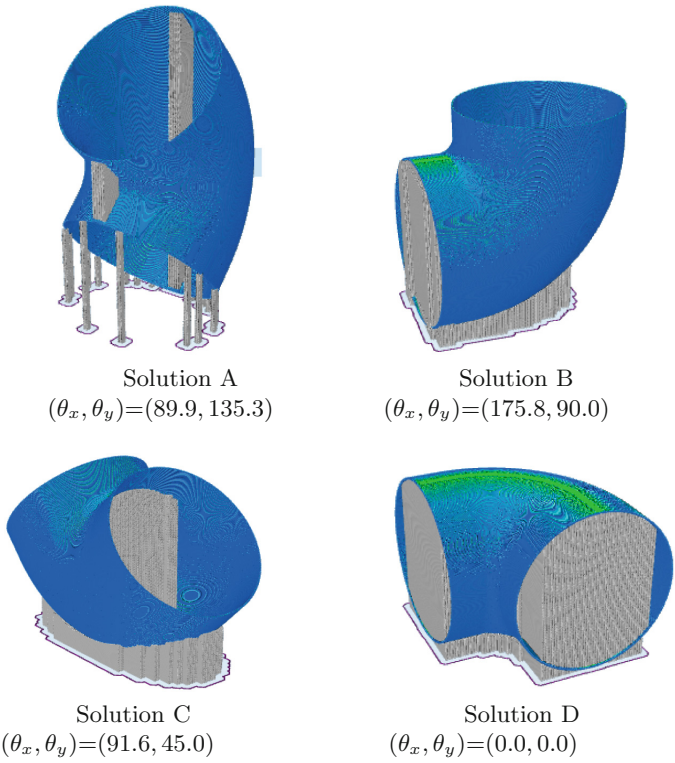

Fig. 11. Representation of the solutions A, B, C and D of 45 Degree Short model.

4 Conclusions and Future Work

In this paper, it is proposed a multi-objective approach to the build orientation optimization problem. The support area and the build time of 3D models are optimized simultaneously. Four building 3D CAD models are studied.

The weighted Tchebycheff scalarization method was used to transform the multi-objective problem into a single-objective one and embedded in the Electromagnetism-like algorithm to solve this multi-objective optimization problem. It is observed that the convexity of Pareto fronts depends on the 3D CAD models being optimized. All Pareto fronts obtained for the 3D models considered have nonconvex regions. This highlights the importance of using a scalarization method that can achieve nonsupported solutions. These results allow us to perceive the relationship between the objectives for each of the models. Moreover, it is possible to identify the trade-offs between the objectives and select the most appropriate solution. Therefore, it is clear the advantage of using a multi-objective approach that considers different criteria to find the best orientation of building 3D CAD models.

For future work, it is intended to apply this approach to multi-objective orientation problems with other criteria and with other more complex models.

Acknowledgments. This work has been supported and developed under the FIBR3D project - Hybrid processes based on additive manufacturing of composites with long or short fibers reinforced thermoplastic matrix (POCI-01-0145-FEDER-016414), supported by the Lisbon Regional Operational Programme 2020, under the PORTUGAL 2020 Partnership Agreement, through the European Regional Development Fund (ERDF). This work was also supported by FCT - Fundação para a Ciência e Tecnologia within the Project Scope: UID/CEC/00319/2019.

References

1. Brika, S.E., Zhao, Y.F., Brochu, M., Mezzetta, J.: Multi-objective build orientation optimization for powder bed fusion by laser. J. Manufact. Sci. Eng. **139**(11), 111011 (2017)
2. Canellidis, V., Dedoussis, V., Mantzouratos, N., Sofianopoulou, S.: Pre-processing methodology for optimizing stereolithography apparatus build performance. Comput. Ind. **57**(5), 424–436 (2006)
3. Canellidis, V., Giannatsis, J., Dedoussis, V.: Genetic-algorithm-based multi-objective optimization of the build orientation in stereolithography. Int. J. Adv. Manufact. Technol. **45**(7–8), 714–730 (2009)
4. Cheng, W., Fuh, J., Nee, A., Wong, Y., Loh, H., Miyazawa, T.: Multi-objective optimization of part-building orientation in stereolithography. Rapid Prototyping J. **1**(4), 12–23 (1995)
5. Dächert, K., Gorski, J., Klamroth, K.: An augmented weighted tchebycheff method with adaptively chosen parameters for discrete bicriteria optimization problems. Comput. Oper. Res. **39**(12), 2929–2943 (2012)
6. Birbil, S.I., Fang, S.-C.: An electromagnetism-like mechanism for global optimization. J. Glob. Optim. **25**, 263–282 (2003)
7. Gurrala, P.K., Regalla, S.P.: Multi-objective optimisation of strength and volumetric shrinkage of fdm parts: a multi-objective optimization scheme is used to optimize the strength and volumetric shrinkage of FDM parts considering different process parameters. Virtual Phys. Prototyping **9**(2), 127–138 (2014)
8. Jaimes, A.L., Martınez, S.Z., Coello, C.A.C.: An introduction to multiobjective optimization techniques. Optim. Polym. Process. 29–57 (2009)
9. Jibin, Z.: Determination of optimal build orientation based on satisfactory degree theory for RPT. In: Ninth International Conference on Computer Aided Design and Computer Graphics, pp. 6–pp. IEEE (2005)
10. Kruth, J.P.: Material incress manufacturing by rapid prototyping techniques. CIRP Ann.-Manufact. Technol. **40**(2), 603–614 (1991)
11. Lan, P.T., Chou, S.Y., Chen, L.L., Gemmill, D.: Determining fabrication orientations for rapid prototyping with stereolithography apparatus. Comput.-Aided Des. **29**(1), 53–62 (1997)
12. Li, A., Zhang, Z., Wang, D., Yang, J.: Optimization method to fabrication orientation of parts in fused deposition modeling rapid prototyping. In: 2010 International Conference on Mechanic Automation and Control Engineering, pp. 416–419. IEEE (2010)

13. Livesu, M., Ellero, S., Martínez, J., Lefebvre, S., Attene, M.: From 3D models to 3D prints: an overview of the processing pipeline. In: Computer Graphics Forum, vol. 36, pp. 537–564. Wiley Online Library (2017)
14. Masood, S., Rattanawong, W., Iovenitti, P.: A generic algorithm for a best part orientation system for complex parts in rapid prototyping. J. Mat. Process. Technol. **139**(1–3), 110–116 (2003)
15. Padhye, N., Deb, K.: Multi-objective optimisation and multi-criteria decision making in SLS using evolutionary approaches. Rapid Prototyping J. **17**(6), 458–478 (2011)
16. Pandey, P., Reddy, N.V., Dhande, S.: Part deposition orientation studies in layered manufacturing. J. Mater. Process. Technol. **185**(1–3), 125–131 (2007)
17. Pereira, S., Vaz, A., Vicente, L.: On the optimal object orientation in additive manufacturing. Int. J. Adv. Manufact. Technol. **98**, 1–10 (2018)
18. Phatak, A.M., Pande, S.: Optimum part orientation in rapid prototyping using genetic algorithm. J. Manufact. Syst. **31**(4), 395–402 (2012)
19. Rocha, A.M.A.C., Pereira, A.I., Vaz, A.I.F.: Build orientation optimization problem in additive manufacturing. In: Gervasi, O., et al. (eds.) ICCSA 2018. LNCS, vol. 10961, pp. 669–682. Springer, Cham (2018). https://doi.org/10.1007/978-3-319-95165-2_47
20. Rocha, A.M.A.C., Silva, A., Rocha, J.G.: A new competitive implementation of the electromagnetism-like algorithm for global optimization. In: Gervasi, O., et al. (eds.) ICCSA 2015. LNCS, vol. 9156, pp. 506–521. Springer, Cham (2015). https://doi.org/10.1007/978-3-319-21407-8_36
21. Steuer, R.E., Choo, E.U.: An interactive weighted tchebycheff procedure for multiple objective programming. Math. Program. **26**(3), 326–344 (1983)
22. Thrimurthulu, K., Pandey, P.M., Reddy, N.V.: Optimum part deposition orientation in fused deposition modeling. Int. J. Mach. Tools Manuf. **44**(6), 585–594 (2004)
23. Wang, W.M., Zanni, C., Kobbelt, L.: Improved surface quality in 3D printing by optimizing the printing direction. In: Computer Graphics Forum, vol. 35, pp. 59–70. Wiley Online Library (2016)